Available online at www.sciencedirect.com

ScienceDirect

Procedia Computer Science 159 (2019) 505–513

Procedia Computer Science

www.elsevier.com/locate/procedia

23rd International Conference on Knowledge-Based and Intelligent Information & Engineering Systems

Automatic wide field registration and mosaicking of OCTA images using vascularity information

Macarena Díaz[a,b,*], Joaquim de Moura[a,b], Jorge Novo[a,b], Marcos Ortega[a,b]

[a] *Faculty of Informatics, Department of Computing, University of A Coruña, A Coruña, Spain*
[b] *CITIC-Research Center of Information and Communication Technologies, University of A Coruña, A Coruña, Spain*

Abstract

Optical Coherence Tomography Angiography (OCTA) constitutes a novel ophthalmological image modality that is characterized for being a non-invasive capture technique that allows a profound analysis of the vascular characteristics of the eye fundus. Given the restricted field of view of the eye fundus that offers each scan, the specialists frequently capture several complementary images that may be simultaneously analyzed to offer a complete and accurate diagnosis of the patient.

In this work, we propose a fully automatic method to register complementary OCTA images and provide compositions for the same patient, generating a wide field of representation that allows a simpler and more direct analysis than the traditional tedious manual procedures. To achieve this, we based our proposal in a robust combination of representative features that are filtered by an accurate identification of the main retinal vasculature. This way, given the characteristic high irregularity in the fundus of the OCTA images, we avoid many variable areas that may interfere in the registration process, restricting the analysis to the most representative and stable structure of this image modality, the main retinal vasculature. In particular, we use *Speeded-Up Robust Features* (SURF) algorithm to extract representative features in the main vascular region that is extracted using a method that combines the analysis of the Hessian matrix followed by an hysteresis threshold process. Then, using a K-NN model, we perform the registration of the resulting features from the different OCTA images to be analyzed. Finally, the *Random sample consensus* (RANSAC) method is exploited to produce the final target mosaic. The proposed method presented satisfactory results in the validation experiments, with accurate values for the MSE index of 1.2566 and 1.6725 pixels for the registration of paired images an mosaics, respectively.

Keywords: Optical Coherence Tomography Angiography, Registration, Mosaicking, SURF, RANSAC, Retinal Vascularity

* Corresponding author. Tel.: +34 981167000.
E-mail address: macarena.diaz1@udc.es

1877-0509
10.1016/j.procs.2019.09.205

1. Introduction

Optical Coherence Tomography Angiography (OCTA) [1] constitutes a recent non-invasive image modality that is characterized by allowing a detailed visualization of the retinal vascularity. The OCTA capture process is based on the identification of the blood flow though the vessels in order to identify these variations using retinal consecutive scans at the same location and time, producing the output OCTA images that highlights the target vascularity. In contrast to the traditional Fluorescein Angiography (FA) [2], OCTA is a non-invasive image modality that could allow the identification of representative biomarkers that are necessary for the diagnosis and monitoring of a large variety of serious vascular pathologies.

In that line, at the moment, different representative clinical studies were published, demonstrating the utility of different biomarkers that may be extracted from OCTA images [3, 4], which may be associated with important pathologies such as diabetic retinopathy [5], retinal vein occlusion [6] or glaucoma [2], among others. In the medical field, and more specifically in ophthalmology, computational automatic approaches and frameworks demonstrated their huge impact and utility in improving and facilitating the expert's work of monitoring and diagnosis of many pathologies [7, 8]. Due to the novelty of the OCTA image modality, there are still few computational proposed approaches, mainly based on the direct extaction of biomarkers [9, 10, 11], and their corresponding analysis. In particular, Díaz *et al.* [9, 10], proposed different methods to measure the vascular density regions in OCTA images as well as to accurately segment the foveal avascular zone. Also, Guo *et al.* [11] proposed a neural network to automatically extract the avascular regions of the OCTA images.

The lack of a wide field representation of the retina is the main disadvantage of individual OCTA images. Given that the capture device extracts a fixed and restricted area of the eye fundus, typically 3×3 or 6×6 millimeters (mm), the visualization of large areas commonly needs more than one overlapping scan to capture all the regions to be studied. This involves a complex and tedious analysis of several separated OCTA images for the same diagnostic process. At present, there are some capture devices that capture larger regions, typically 12×12 mm, but still representing low values and presenting important disadvantages. In particular, given that the extraction process is in a larger area, the detail level is significantly lower, being also the quality of the image poorer. Moreover, the vessels appear more blurred as well as more noisy artifacts are present in the output image given the imprecise acquisition process. For these reasons, the specialists typically prefer the use of more restricted fields of view, capturing several overlapping OCTA images. This approach is benefited from the quality of OCTA images with higher zoom level, presenting less artifacts and a higher level of details, but hardening the diagnostic process with the simultaneous analysis of the required complementary OCTA images. In this context, the automatic availability of a complete mosaic, registering the images, is extremely useful to facilitate and fasten the revision process of the specialists.

At this moment, this approach is scantly used in OCTA imaging. In fact, there is only one work that deals with this complex issue in the state of the art. Thus, Wang *et al.* [12] proposed a method to solve the explained composition problem using the *Speeded-Up Robust Features* (SURF) algorithm to directly extract accurate keypoints and descriptors from the entire raw OCTA images. Then, with these features and the *Random sample consensus* (RANSAC) algorithm, the composition is achieved. The main limitation of the OCTA images is the significant level of noise and the background irregularity that are produced by the capture process and the retinal tissues that may interfere in the identification of representative keypoints to be aligned. For that reason, the registration process in this image modality constitutes a more challenging issue than in other practical domains.

Hence, in this work, we propose an accurate and improved method that combines the robust extraction of keypoints using SURF but being conditionated by the main representative characteristic of the OCTA images: the main retinal vessel tree. This way, we guarantee the identification of usefull keypoints, avoiding the detection of keypoints in many noisy regions that may confuse the registration process. Firstly, we extract the vessels using an approach that analyzes the Hessian matrix followed by a hysteresis based threshold to extract the vascular regions [13]; then, we exploit the identified vascular information to restrict the extraction of the keypoints and descriptors with SURF and assemble the target mosaic with RANSAC.

This paper is organized as follows: in Section 2, we explain the proposed methodology to register the OCTA images and produce the target mosaics; in Section 3, the designed experiments to validate and compare the method as well as the obtained results are presented and explained; finally, in Section 4, we discuss the obtained results and compare them with the state of the art.

Fig. 1: Main steps of the proposed methodology.

2. Methodology

The proposed methodology, represented in Fig. 1, is divided into four main steps. First, a preprocessing stage is applied to the input OCTA image to facilitate the posterior stages of the proposed method. Second, the vessel extraction is performed to filter the representative useful vascular regions of the OCTA images. For this second step, we use a method [13] that was specifically adapted to the characteristics of this problematic. Then, the keypoints and descriptors are extracted using the SURF algorithm, being exploited in different alternative approaches: first, these features are extracted from the original image, following the state of the art and that will be serve as comparison to motivate the utility of using the vascular region; and second, the extraction of these features is performed on the preprocessed OCTA image, being preserved only those from the extracted vessel regions. Finally, with the extracted features, the registration process is performed to reach the target mosaic. The Mean Square Error (MSE) metric is employed to measure the performance of the registration process.

2.1. Image preprocessing

OCTA images are characterized by a bright irregular noise over the dark background. As said, this noise could affect the extraction of the keypoints in the application of SURF. For this reason, we designed a preprocessing step where the target noise is reduced. Due to the constitution of this noise, we decided to apply a morphological top hat operator followed by a median filter [14]. Hence, with the morphological top hat operator, we enhance the vessels over the background; and with the median filter, the noisy pixels are reduced by the median of the neighborhood, smoothing briefly the OCTA image but preserving the mains structures over the OCTA image. Figs. 2 (b) and (f) show illustrative examples of application of this step.

2.2. Vessel extraction

As said, in this methodology, we use the main vascularity information to restrict the analysis to the relevant areas of the image and avoid other problematic noisy and variable regions. For this reason, we need to segment the vessels from the input OCTA image and construct the mask based on this extraction to be posteriorly used in the keypoints identification process. To make this vascular segmentation, we based our proposal in the work that was proposed in [13], being specifically adapted to this new challenging scenario. This vessel segmentation is mainly based on a enhancement of the vascularity using the Hessian matrix followed by an hysteresis based thresholding process to segment the previously enhanced vessels. Once the vessels are extracted, the method removes isolated points, product of the previous segmentation process. Additionally, before the application of the subsequent steps of the methodology, we apply a morphological dilation operator to obtain an inclusive region with a vessel mask that also complementary includes the surrounding information of the vessels and not only the restricted main pixels of these vessels. Figs. 2 (c), (d), (g) and (h) present representative examples of application of this stage.

2.3. Extraction of the keypoints and descriptors

Using the preprocessed OCTA image and its extracted vascular structure, we proceed with the identification of the representative keypoints and their descriptors to, posteriorly, perform the registration process of the OCTA images and produce the final mosaic. In particular, two different approaches were implemented and tested in this stage:

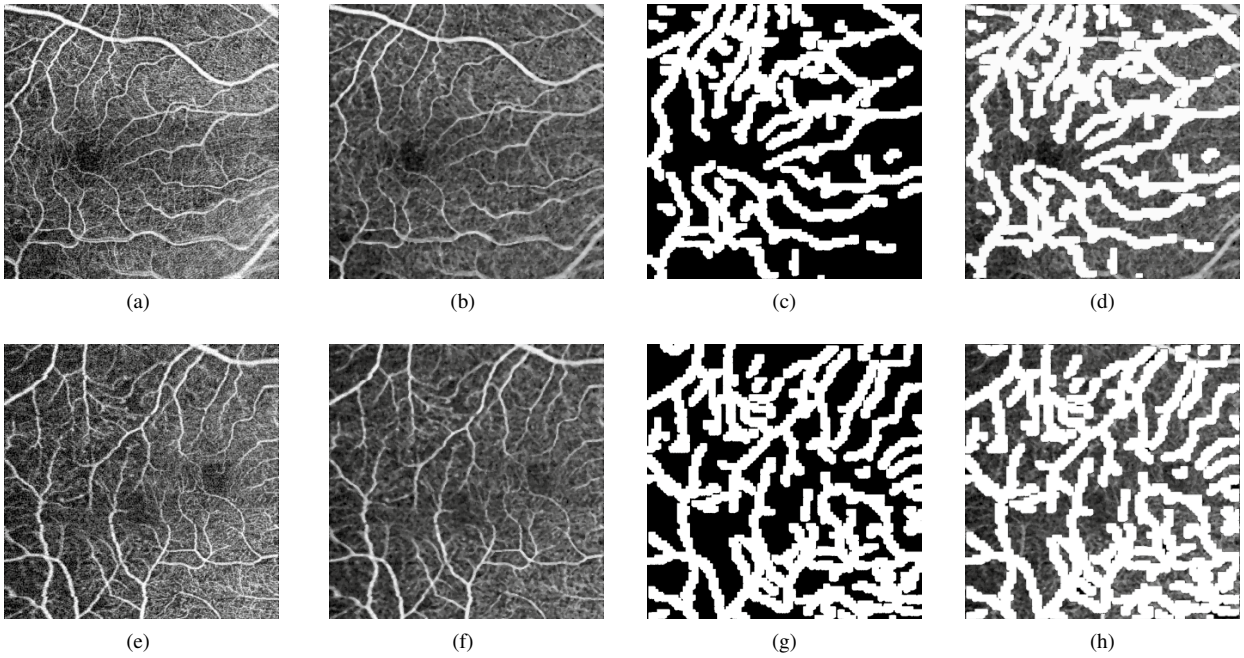

Fig. 2: Preprocessing and vascular extraction stages. (a) and (e) Input OCTA images. (b) and (f) Image results after applying the top hat operator and the median filter. (c) and (g) Image results after applying the vessel extraction process. (d) and (h) Vessels extracted and dilated superposed to the input OCTA image.

- *Approach 1*: we extract the keypoints and their descriptors directly in the preprocessed OCTA image. This approach is in line with the proposal of the state of the art [12], but being applied in our case over the enhanced image.
- *Approach 2*: we extract the keypoints and descriptors in the preprocessed OCTA image, but conditioning their identification to the extracted vascular region.

In both cases, the SURF algorithm [15] was used to find the representative keypoints and their corresponding descriptors. This algorithm is characterized by their invariability with the pixel values, scaling and rotating, as well as a fast and robust performance. This presents important advantages that make this algorithm suitable for this image modality, also being previously applied in this issue [12]. In Fig. 3, we can see representative examples of the keypoints extraction process using each described approach.

2.4. OCTA image registration

The composition process is performed by the progressive pairing of new input OCTA images to the resultant mosaic. The following subsections depict this process in detail.

2.4.1. Exhaustive search

Given that these input OCTA images can be paired in different order, and consequently produce different results, we decided to prioritize then with the best registration order. To do this, we performed an exhaustive search of the best possible registration of paired images with the smallest value of MSE. In particular, given that the registration process is characterized by having a fixed image and a moving image that is transformed, the order of the OCTA image selection affects to the result of the final mosaic. For this reason, to guarantee the best possible result, we explore all the permutations of fixed and moving image.

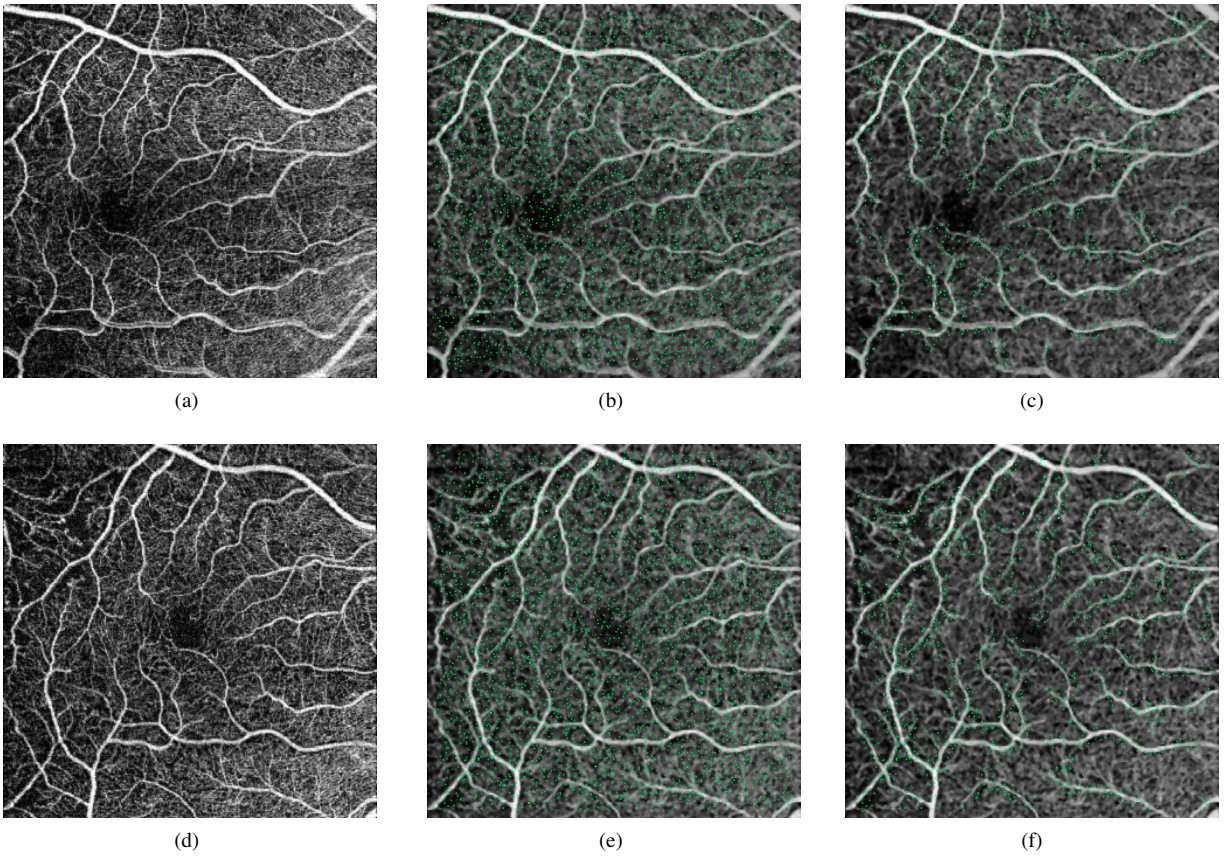

Fig. 3: Examples of the keypoint extraction process using each approach. (a) and (e) Original image. (b) and (f) Keypoints extracted using the entire preprocessed OCTA image. (c) and (g) Keypoints extracted used the preprocessed OCTA image and filtered with the vascular extracted mask.

2.4.2. *Matching keypoints in the images*

To make the posterior registration, we need to know the correspondence between the identified keypoints of each image. To perform this matching, we use the k-Nearest Neighbors (K-NN) [16] algorithm, finding the keypoint correspondence by analyzing the similarities between their descriptors. With this step, each keypoint of one image is connected with a keypoint in the other image.

2.4.3. *Paired image registration*

Once we know what are the correspondences between the keypoints of both images, we need to find the Homography matrix that provides the necessary perspective transformation for the moving image. This transformation is obtained using RANSAC [17]. RANSAC is a non determinist algorithm that selects paired points and search for the best transformation between them. With this transformation based on the selected paired points, it is necessary to check if the whole paired points are matched between them. RANSAC tests with different sets of paired points and transformations and selects the best configuration, extracting its Homography matrix. With the extracted Homography matrix, we apply the transformation to the moving image that is joined with the fixed image, obtaining therefore the resultant paired output image. In Fig. 4, we can see an example of application of this step.

2.4.4. *Final mosaic construction*

The resultant paired image is used as the new fixed image containing the method with the search of the best registration with the remaining input OCTA images. This step is repeated until all the images are aggregated to the constructed output mosaic.

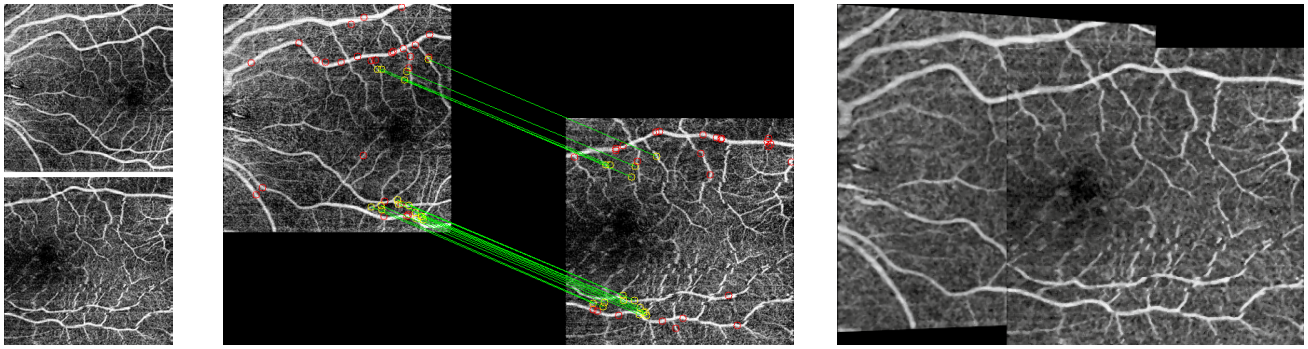

(a) (b) (c)

Fig. 4: Example of application of the K-NN step. (a) Input images. (b) Paired points between the input images. (c) Final mosaic result.

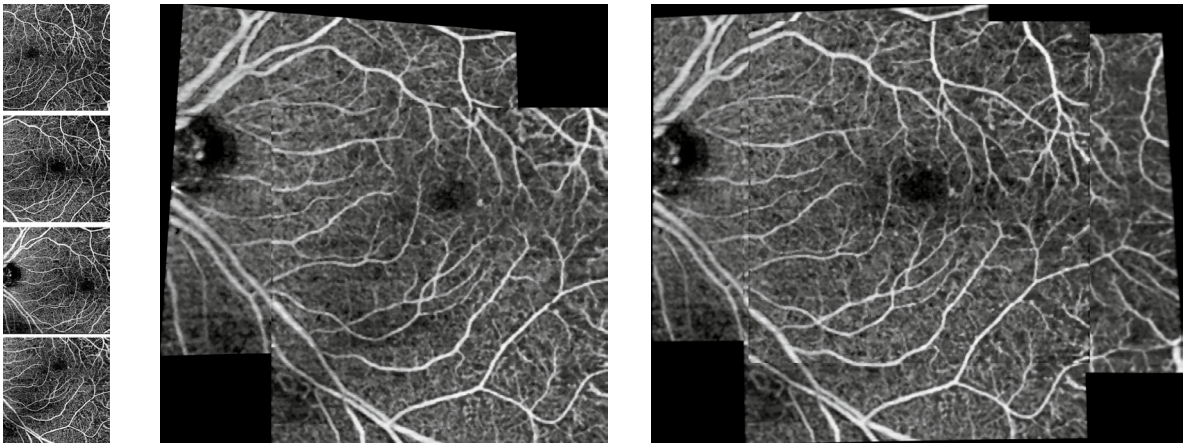

(a) (b) (c)

Fig. 5: Example of application of the paired image registration and production of the final OCTA mosaic. (a) Input images. (b) Example of paired images. (c) Final OCTA mosaic.

3. Experimental Results

To prove the suitability of the proposed method, we used a complete and heterogeneous set of OCTA images and different validation experiments that were applied to this dataset. All the tests were made with both approaches that were explained before, comparing their results to perform the analysis and reach the conclusions, in Section 4, of this work.

3.1. Image dataset

The used dataset contains several OCTA images that were captured from 10 patients. In particular, they present a resolution of 6×6 mm in superficial plexus for left and right eyes. Each eye include 3 or 4 images from the macular area, temporal area and center area. Summarizing, we have a total of 54 OCTA 6×6 mm images at superficial plexus. These OCTA images were taken using the Optical Coherence Tomography capture device DRI OCT Triton; Topcon Corp, with a resolution of 320×320 pixels. Having in mind the 3 or 4 images per eye of 10 patients, we could perform the different experiments over individual pairs of overlapping images as well as over complete OCTA mosaics. In particular, we retrieved 19 mosaics and 49 overlapping image pairs.

3.2. Validation

To measure the performance of the method, we used the Mean Square Error (MSE) [18] metric that is commonly used in similar validation processes. In particular, with the MSE metric, we can measure the distances between the positions of the keypoints and their ideal positions. This measurement is made with the indexes of the keypoint positions in the moving images after its transformation and the indexes of the keypoints in the fixed images. We calculated the MSE measurement in each registration as follows:

$$MSE = \frac{1}{N}\sum_{i=0}^{N}(\hat{Y}_i - Y_i)^2 \tag{1}$$

where Y contains the original points (x,y) of the fixed image and $\hat{Y}$ indicate the points $(\hat{x}, \hat{y})$ obtained with the transformation in the moving image.

In Table 1, we can see the obtained results using the MSE metric with each approach over the entire used image dataset. Hence, we calculated the MSE measurement over the paired images as well as the complete mosaics. In this second scenario, we computed the global MSE of the mosaic as the average of each registered image to the global mosaic. Additionally, we converted the calculated MSEs values in pixels to mm, to know the real impact of this error in the real scale of the eye fundus.

As said, we tested both explained approaches. The first one is in line with the state of the art, but being applied over the preprocessed images herein presented, baseline for comparison with the vascular approach. The second approach include the alternative strategy, filtering the region of interest and analysis by the main retinal vessel tree.

Generally, both approaches provided satisfactory results, returning mean MSE values that are significantly low, in terms of pixels and mm, given the analyzed resolutions. Additionally, as we can see, the second approach improves significantly the results of the basic alternative. This is motivated by the explained concept that the general background of the OCTA images is highly irregular and may alter significantly from over scan to another. In contrast, the main retinal vessel tree is stable, being the keypoints more representative and similar between scans. Therefore, those keypoints are more robust and desirable to find the registration between overlapping OCTA images.

Table 1: MSE results using each presented approach.

Approach	Paired images		Mosaics	
	MSE	Offset	MSE	Offset
1	2.1463 px	40.2431 μm	2.1296 px	39.9300 μm
2	1.2566 px	23.5612 μm	1.6725 px	31.3593 μm

4. Discussion and Conclusions

A significative variety of pathologies affects directly the retinal micro-circulation, being a sensitive part of the whole circulatory system, not only for diseases of the eye but also for other systemic ones. Thus, hypertension or diabetes and others as glaucoma may produce vision impairment, even deriving in irreversible blindness in their final stages. However, their early identification and diagnosis could prevent this drastic consequences.

In ophthalmology, as in many other medical domains, it is very common the use of different image modalities to support the clinical procedures of diagnosis and monitoring. Among them, OCTA imaging is the most recent modality, being characterized by a non invasive and quick extraction process, which is more comfortable and less invasive for the patients. This image modality allows the visualization of the retinal vasculature, as its predecessor, the fluorescein angiography, but non-invasively, providing a great improvement. Due to the novelty of the OCTA images, there are still few clinical studies that demonstrate their utility, specially in comparison with other consolidated ophthalmological image modalities, like the color fundus retinography or the mentioned fluorescein angiography. All the studies are significantly recent, still appearing new ones that demonstrate the potential uses of the OCTA images. The main

inconvenience of the OCTA image modality is that the captured and represented region of the eye fundus is typically short, with dimensions of 3×3 or 6×6 mm in most of the used cases. In order to improve the analysis of the OCTA images in the diagnostic procedures, it is desirable a greater wide field of representation.

For this reason, it is proposed in this work the automatic registration of complementary OCTA images and the subsequent construction of retinal OCTA mosaics, providing accurate results. The proposal firstly implements a pre-processing stage, applying a top hat operator to enhance the vessels as well as a median filter to reduce the background noise of the OCTA images. Then, the method exploits the robust properties of the SURF algorithm to extract representative keypoints and descriptors that are necessary to make the posterior registration. Given the high complexity and the significative background irregularity of the OCTA images that is produced by capture imperfections and the retinal tissues, the general extraction of the keypoints using SURF is combined with the analysis of domain related characteristics. In particular, the keypoints are restricted to the main retinal vessel tree, the main structure of the eye fundus, specially visible in the OCTA images and that is stable over different capturing processes. Using K-NN, we find the matches of the keypoints between the images to, posteriorly, construct the desired registration with the RANSAC method. In general terms, the proposal offers an accurate performance in terms of the analysis using the MSE metric, outperforming the general application of using directly the entire image.

As future work, we propose an extension of the analyzed dataset by including other typically used configurations as deep plexus OCTA images, which are characterized by their difficulty based on the absence of main vessels that are typically present in superficial plexus. With these images, we propose the adaptation of the proposed method to the particular characteristics of this configuration of OCTA image. Hence, we also intend the inclusion of 3×3 mm OCTA images to obtain mosaics with a higher quality level; also 12×12 mm OCTA images may be studied to obtain a larger vision and complement the doctor's work of analyzing and monitoring different vascular diseases.

Acknowledgements

This work is supported by the Instituto de Salud Carlos III, Government of Spain and FEDER funds of the European Union through the DTS18/00136 research projects and by the Ministerio de Economía y Competitividad, Government of Spain through the DPI2015-69948-R research project. Also, this work has received financial support from the European Union (European Regional Development Fund - ERDF) and the Xunta de Galicia, Centro singular de investigación de Galicia accreditation 2016-2019, Ref. ED431G/01; and Grupos de Referencia Competitiva, Ref. ED431C 2016-047.

References

[1] de Carlo, T.E., Romano, A., Waheed, N.K., Duker, J.S., 2015. A review of optical coherence tomography (OCTA). International Journal of Retina and Vitreous 1.

[2] NOVOTNY, H.R., ALVIS, D.L., 1961b. A Method of Photographing Fluorescence in Circulating Blood in the Human Retina. Circulation 24, 82–86. URL: https://www.ahajournals.org/doi/10.1161/01.CIR.24.1.82, doi:10.1161/01.CIR.24.1.82.

[3] Feucht, N., Maier, M., Lepennetier, G., Pettenkofer, M., Wetzlmair, C., Daltrozzo, T., Scherm, P., Zimmer, C., Hoshi, M.M., Hemmer, B., Korn, T., Knier, B., 2019. Optical coherence tomography angiography indicates associations of the retinal vascular network and disease activity in multiple sclerosis. Multiple Sclerosis Journal 25, 224–234. URL: http://journals.sagepub.com/doi/10.1177/1352458517750009, doi:10.1177/1352458517750009.

[4] Tang, P.H., Jauregui, R., Tsang, S.H., Bassuk, A.G., Mahajan, V.B., 2019. Optical Coherence Tomography Angiography of RPGR -Associated Retinitis Pigmentosa Suggests Foveal Avascular Zone is a Biomarker for Vision Loss. Ophthalmic Surgery, Lasers and Imaging Retina 50, e44–e48. URL: https://www.healio.com/doiresolver?doi=10.3928/23258160-20190129-18, doi:10.3928/23258160-20190129-18.

[5] Hwang, T.S., Gao, S.S., Liu, L., Lauer, A.K., Bailey, S.T., Flaxel, C.J., Wilson, D.J., Huang, D., Jia, Y., 2016. Automated Quantification of Capillary Nonperfusion Using Optical Coherence Tomography Angiography in Diabetic Retinopathy. JAMA Ophthalmology 134, 367. URL: http://archopht.jamanetwork.com/article.aspx?doi=10.1001/jamaophthalmol.2015.5658, doi:10.1001/jamaophthalmol.2015.5658.

[6] Balaratnasingam, C., Inoue, M., Ahn, S., McCann, J., Dhrami-Gavazi, E., al. Yannuzzi, L.A.b., 2016. Visual Acuity Is Correlated with the Area of the Foveal Avascular Zone in Diabetic Retinopathy and Retinal Vein Occlusion. American Academy of Ophthalmology 123.

[7] Novo, J., Rouco, J., Barreira, N., Ortega, M., Penedo, M.G., Campilho, A., 2017b. Hydra: A web-based system for cardiovascular analysis, diagnosis and treatment. Computer methods and programs in biomedicine 139, 61–81.

[8] Novo, J., Hermida, A., Ortega, M., Barreira, N., Penedo, M.G., al. López, J.E.b., 2017a. Wivern: a Web-Based System Enabling Computer-Aided Diagnosis and Interdisciplinary Expert Collaboration for Vascular Research. Journal of Medical and Biological Engineering 37, 920–935.

[9] Díaz, M., Novo, J., Cutrín, P., Gómez-Ulla, F., Penedo, M.G., Ortega, M., 2019. Automatic segmentation of the foveal avascular zone in ophthalmological OCT-A images. PLOS ONE 14, e0212364. URL: http://dx.plos.org/10.1371/journal.pone.0212364, doi:10.1371/journal.pone.0212364.

[10] Díaz, M., Novo, J., Penedo, M.G., Ortega, M., 2018. Automatic extraction of vascularity measurements using OCT-A images. Procedia Computer Science 126, 273–281. URL: https://www.sciencedirect.com/science/article/pii/S1877050918312377, doi:10.1016/J.PROCS.2018.07.261.

[11] Guo, Y., Camino, A., Wang, J., Huang, D., Hwang, T.S., Jia, Y., 2018. MEDnet, a neural network for automated detection of avascular area in OCT angiography URL: https://doi.org/10.1364/BOE.9.005147, doi:10.1364/BOE.9.005147.

[12] Wang, J., Camino, A., Hua, X., Liu, L., Huang, D., Hwang, T.S., Jia, Y., 2019. Invariant features-based automated registration and montage for wide-field OCT angiography. Biomedical Optics Express 10, 120. URL: https://www.osapublishing.org/abstract.cfm?URI=boe-10-1-120, doi:10.1364/BOE.10.000120.

[13] Calvo, D., Ortega, M., Penedo, M.G., Rouco, J., 2011. Automatic detection and characterisation of retinal vessel tree bifurcations and crossovers in eye fundus images. Computer Methods and Programs in Biomedicine 103, 28–38. URL: https://www.sciencedirect.com/science/article/pii/S0169260710001446, doi:10.1016/J.CMPB.2010.06.002.

[14] Thompson, B.J., 1992. Mathematical Morphology in Image Processing. CRC Press. URL: https://www.taylorfrancis.com/books/9781482277234, doi:10.1201/9781482277234.

[15] Bay, H., Tuytelaars, T., Van Gool, L., 2006. SURF: Speeded Up Robust Features, Springer, Berlin, Heidelberg, pp. 404–417. URL: http://link.springer.com/10.1007/11744023{_}32, doi:10.1007/11744023_32.

[16] Cover, T., Hart, P., 1967. Nearest neighbor pattern classification. IEEE Transactions on Information Theory 13, 21–27. URL: http://ieeexplore.ieee.org/document/1053964/, doi:10.1109/TIT.1967.1053964.

[17] Fischler, M.A., Bolles, R.C., 1981. Random sample consensus: a paradigm for model fitting with applications to image analysis and automated cartography. Communications of the ACM 24, 381–395. URL: http://portal.acm.org/citation.cfm?doid=358669.358692, doi:10.1145/358669.358692.

[18] Su, M., Zhang, C., Chen, Z., Jiang, S., 2017. Registration of multimodal brain images based on optical flow, in: 2017 10th International Congress on Image and Signal Processing, BioMedical Engineering and Informatics (CISP-BMEI), IEEE. pp. 1–5. URL: http://ieeexplore.ieee.org/document/8302198/, doi:10.1109/CISP-BMEI.2017.8302198.